Reuse Partitioning and System Capacity in the Adaptive OFDM Downlink of the Wireless IP Project Target System

Mikael Sternad[1]
[1] Signals and Systems, Uppsala University, Box 528, SE-75 120 Uppsala, Sweden

Version 3.1, 7th July 2003

Abstract

How can we, in our proposed adaptive OFDM downlink, simultaneously obtain good coverage within cells and a high average spectral efficiency? The present report outlines a solution to this problem. It also gives a first estimate of the attainable system capacity for our target radio interface. The proposed method uses coordinated scheduling among sectors on the same site (radio access point) to suppress interference. Furthermore, one frequency band (with reuse 1) transmits to near users, while another band, with orthogonal resource sharing among clusters of 3 base stations, transmits to far-off users in the sectors. The key idea is to apply a frequency reuse factor > 1 only where it is needed most, in the outer part of the sector, where the signal from the base station is weak. It becomes possible to attain coverage over the whole sector, with an effective resource reuse 2 and an average capacity of 1.24 bit/s/Hz/sector for one Rayleigh fading user, including overhead, without assuming multiuser diversity or multiple receiver antennas. At least 16-QAM can be used in $\approx 33\%$ of the sector area. The resulting signal-to-interference ratio and spectral efficiency has been evaluated as a function of the position within the sector, by summing over all relevant interferers. The traffic density is assumed constant over the area, and hexagonal coverage areas are assumed for the base stations. Both triangular 60^o sectors and diamond-shaped (30^o rotated) sectors are considered. The antenna pattern and an exponential path loss is taken into account. The spectral efficiency is first calculated for one user per sector (no multiuser diversity) with adaptive modulation. Results are presented for static channels and for flat Rayleigh-fading channels, both with path-loss. Situations with K active users within the sectors who each have L antennas and use maximum ratio combining are then investigated, for Rayleigh fading channels with path loss. The presented estimates neglect shadow fading and noise. They therefore represent only a first approximation of the true, much more complicated, situation, which we will investigate in our system simulator under construction. Various ways of improving this basic solution are discussed briefly, including the use of coordinated scheduling over several base stations, slow power control, the use of interference rejection by multiple antennas in user equipment, and transmission by Trellis-coded adaptive modulation instead of uncoded adaptive modulation. The methods and performance measures presented here can serve as benchmarks for such more elaborate solutions.

Contents

1 Introduction 3

2 Outline of the Investigated Strategies 3

3 Scheduling Between Sectors 6

4 Resource Sharing Within Zone 2 7

5 The SIR due to Path Loss and Interference 9

6 Deterministic Estimate of the Spectral Efficiency 14

7 Optimization of Zone Border (Deterministic Case) 18

8 Spectral Efficiency for One Rayleigh Fading User 20

9 Average Sector Capacity for K Users with L Antennas, Path Loss and Rice Fading 24

10 Summary of Sector Capacity Results 26

11 Conclusions and Open Issues 28

1 Introduction

The Wireless IP project [1] studies problems that are important in the evolution of UMTS toward higher data rates, as well as in future technologies for mobile systems beyond 3G. Our goal is to improve the spectral efficiency for packet data, in particular IP traffic, with sufficient quality of service for various traffic classes.

We have in [2] outlined a radio interface that aims at providing high data rates. It should attain high spectral efficiency, handle mobile users up to 100km/h, and offer wide area coverage *simultaneously*. The present report discusses methods for interference avoidance and scheduling between sectors that lead to good signal to interference ratios (SIRs) and also to a reduction of the variability of the SIR with the location within sectors. These techniques are crucial for obtaining high spectral efficiency and wide area coverage (as opposed to only hot-spot coverage). We also provide a first estimate of the system capacity that may be expected, for static channels and for Rayleigh fading channels.

In the proposed hypothetical 4G system, we at present assume FDD, i.e separate frequency bands for uplinks and downlinks. A base station infrastructure and a tight reuse of the bandwidth is assumed. Within sectors of each base station, the transmission is performed by an adaptive OFDMA scheme. For example, a 5MHz bandwidth is partitioned into 500 subcarriers, of which bins of 20 (200kHz) are allocated to users during time-slots of length 0.666ms. The allocation of time-frequency bins is performed by a scheduler at the base station. It is based on feedback information on the predicted channel quality in each slot, computed by each mobile. The transmission uses a modulation format appropriate for the target bit error rate for the intended user for a particular channel. BPSK and QAM formats, from 4QAM up to 256QAM, may be used. High spectral efficiency is to be attained by a combination of multiuser diversity, link adaptation, use of MIMO channels and strategies for interference suppression and interference avoidance.

2 Outline of the Investigated Strategies

We assume radio access points (base stations) at fixed locations that all utilize the same spectral band of width s_0.

To estimate the spectra efficiency, we will first use a deterministic approach with a continuous user distribution. A basic simplifying assumption is that

The number of active users per unit area is constant over the considered area.

It is then reasonable to assume the locations (sites) of the base stations to be regularly spaced. We here assume a conventional *hexagonal pattern*, see Figure 1.

The *coverage area* of a base station is defined as the areas where the signal is strongest from that particular station. The coverage areas will be hexagonal. The coverage areas are partitioned into N_s *sectors*, also called *lobes* or *cells*. We may in general assume the beam-widths and lobe directions to be adjusted slowly, to adapt to traffic variations within the coverage area. An equal number of active users within each lobe could be a reasonable criterion for the adaptation. With the above assumption of constant traffic density, all lobes will then, on average, have equal width $360/N_s$ deg. We here assume $N_s = 6$ sectors of equal fixed width 60^o and side length R at all sites. The signal-to-interference ratio in one of these sectors (the triangle pointing to the right from the origin in Figure 1) will be investigated in detail, by taking interference from the 36 first, second and third-tier interferers (within radius 5.5R) into account. More distant interferers and noise will be neglected in the analysis.

We will consider the *triangular sector* shown by Figure 1 and the lower part of Figure 2. Note that the closest interferer (at $x = 1.73R$) will then also have a triangular sector, beaming along the negative x-axis into our sector. A *diamond-shaped sector*, obtained by shifting the sector by 30^o within the hexagon, is also considered, see the upper part of Figure 2. We then obtain a 60^o analog of the Ericsson cell plan for 120^o sectors, in which close-by sectors do not point directly towards each other. Its consideration was inspired by the report [5].

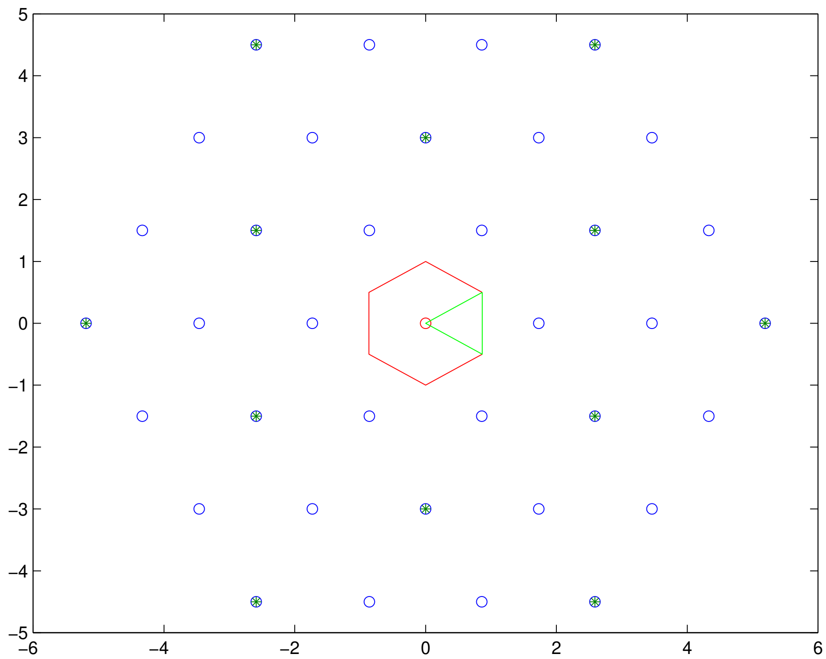

Figure 1: The hexagonal site pattern. Base stations which have 6 sectors/lobes are located at the indicated positions. There are 37 base stations, having 222 sectors (or cells). "Our" base station, with the red hexagonal coverage area, is at the origin. The sector of interest is in this case triangular and directed toward the positive x-axis. Rings represent all base stations that are taken into account in the analysis of the interference. Noise and interference from outside of this area is neglected. When transmitting to the outer parts of sectors, a reuse 3 pattern of groups of 3 sites is used. The sites in this pattern that transmit simultaneously with our site, and thus cause interference, are indicated by crossed rings.

Interference is reduced in this system by three strategies. The first two accomplish a large interference reduction, at the price of a modest reduction of the maximal number of usable time-frequency bins per site.

- To reduce interference from adjacent sectors of "our" site, the scheduler will order the neighboring sectors to abstain from using time-frequency bins that

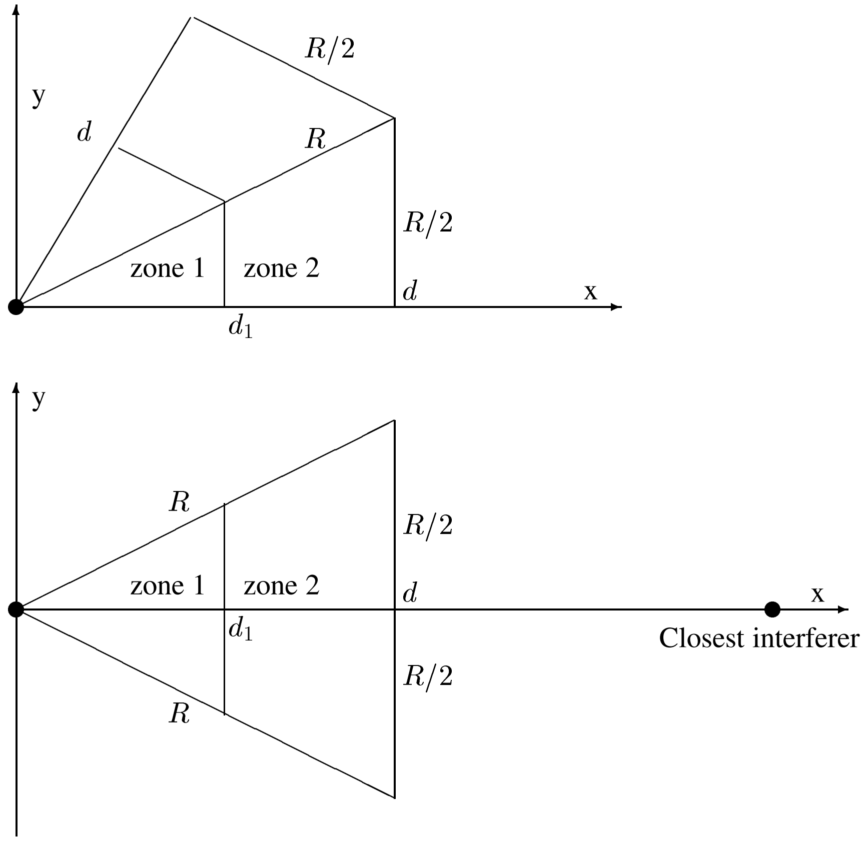

Figure 2: Enlargements of the two types of 60^o sectors considered. A diamond-shaped sector, with center direction $+30^o$ is shown in the upper figure, while a triangular sector is shown in the lower figure. We use frequency reuse 1 of the frequency band s_1 in zone 1, while the frequency band s_2 is allocated to the outer zone 2, where it is shared over 3-site groups in a reuse 3 pattern. (Note that the figure is not exactly to scale, due to restrictions in the Latex line-drawing function.)

are allocated to users in our sector that are close to the site boundary (within an angle β from the boundary). Likewise, our sector will not transmit during bins that are allocated to such *border users* in neighboring sectors. This scheduling between sectors is discussed in more detail in Section 3 below.

- When transmitting to distant users within the sector (beyond distance d_1 in what is denoted zone 2 of the sector, see Figure 2), we use a separate part of the total frequency band s_0 that will be denoted s_2. We there use reuse partitioning 3, i.e sites are grouped into clusters where each site is given exclusive access to 1/3 of the resource. The reuse pattern is synchronized over all sites, as in present FDMA/TDMA systems. This strategy will radically improve the SIR within zone 2. It will also help to equalize the perceived SIR within the sector, and increase the modulation levels that can be used when transmitting to distant users, close to the outer cell boundary. The switching distance $d_1 \leq d$ is the main system parameter. It is studied and optimized in Sections 4-7 below.
- Multiple antennas in mobiles, can further improve the SIR significantly. In the first sections of this report, only a single omni-directional antenna is as-

sumed at each user terminal. In Section 9, the use of maximum ratio combining with $L \leq 4$ antennas is evaluated. This is the result that can be expected if the interference arrives isotropically, from all directions. With few dominant propagation paths and interference with clear directionality, interference rejection combining (IRC) can further improve the SIR significantly. That is an aspect for future studies. The potential of MIMO transmission over two transmit branches to two receivers has been discussed in [4].

3 Scheduling Between Sectors

The assumed antenna radiation power azimuth pattern of the 60^o sector antenna is shown in Figure 3. It consists of a scaled sinc pattern, with sidelobes damped by more than 30dB. The transmit power is normalized to 0 dB at the sector center (angle $\theta = 0^o$) and it has been scaled to decrease to -8.1dB at $\theta = 30^o$. The 3 dB beam-width is 39^o. The lobe creates significant interference in the neighboring sector (angle $\theta > 30^o$), but the power decreases rapidly with increasing angle.

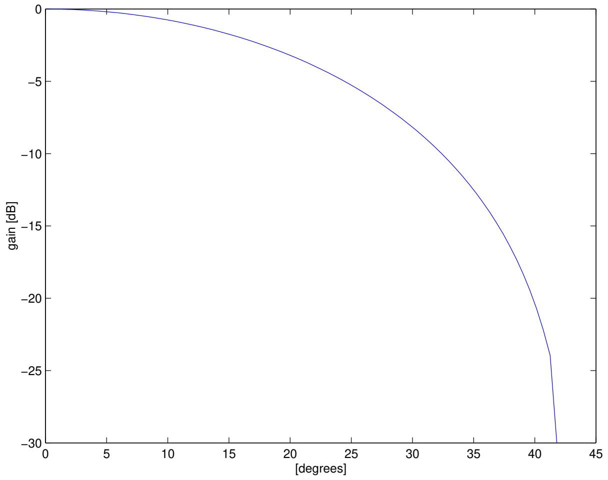

Figure 3: The assumed antenna radiation power azimuth pattern, normalized to 0 dB at zero degrees, with the sector boundary being at 30^o.

To boost the power close to the cell boundary and reduce the interference in neighboring sectors, we suggest the following strategies, which are an elaboration of our original proposals in [2] for scheduling between sectors:

- When transmitting to a *border user* within β degrees from the cell boundary ($30^o - \beta < \theta < 30^o$), the transmit power of that time-frequency bin is boosted by a factor 2 (3 dB). This reduces the variation of the received power as a function of the angle.
- When transmitting to border users, the neighboring sector will not be allowed by the scheduler to use the same time-frequency bin.[1] This strategy is

[1] Information exchange represents no problems, since all sectors belong to the same base station. The design of a scheduling algorithm that can take the above described constraint into account without many rounds of iterative re-scheduling is a topic for current research, e.g for Nilo.

more efficient than a soft-handover strategy of letting both sectors transmit the same information in the same bin with the normal power level .[2]

We thus completely eliminate interference where it would be most severe, close to the sector boundary. If $\beta < 12^o$, we do have some remaining interference around angle 40^o (10^o inside the neighboring sector), for the antenna gain pattern of Figure 3.

We will in the following use $\beta = 7.5^o$ as default value. This corresponds to 25% of the area of the 60^o sector.

The proposed coordinates exclusive scheduling corresponds to a frequency reuse factor 2 for the fraction of resources utilized by border users. The angle β is a system parameter which balances the capacity loss due to exclusive transmission against the remaining interference level generated in the neighboring sector. The resulting capacity reduction due to the scheduling constraint is

$$c_1 = 1 - \frac{1}{2}\frac{\beta}{30^o} = \frac{7}{8} \tag{1}$$

for $\beta = 7.5^o$. Optimization of β for a given antenna pattern should be straightforward, but is left for future research.

When calculating the interference from the neighboring sites, the angle with respect to the cells of the interferer is calculated and the angle-dependent total overlapping radiation pattern of the antenna is taken into account. The assumed 3dB power boost during $\beta/30 = 25\%$ of the time is (for fully loaded cells) canceled by the fact that the neighboring cell is prevented from transmitting. It is therefore neglected in the calculation of the interference power.

4 Resource Sharing Within Zone 2

When transmitting to users in the outer part of the sector (zone 2), we assume a constant transmit power (the same that is used for the inner zone), except for border users, where the power is increased by a factor 2, as described above. In zone 2, we use the part s_2 of the total allocated spectral bandwidth s_0, while the fraction s_1 is allocated to the inner zone 1 of the sector. All the sectors of "our" base station are simultaneously allowed exclusive use of $1/3$ of the resource s_2, on average over time. The resource is shared among clusters of three sites, in a classical reuse 3-pattern. This *orthogonal resource sharing* can be realized by spectral partitioning, time division or a combination of both.[3] If the same strategy is used at all sites, *and* if we assume that the spectral bandwidth s_2 allocated to the distant users is the same at all sites, we may calculate the resulting capacity

[2]Simultaneous transmission is equally effective as coordinated exclusive scheduling only when the user is at the precise border between the sectors, where the signal strengths are equal. For locations with unequal signal strengths from the two sectors, the sum of the power is always less than if the power of the strongest path is doubled while the weaker path is set to zero.

[3]Finding the best strategy for resource sharing is an interesting research sub-problem: A fixed partitioning of s_2 into three sub-bands of equal width will reduce the spectral diversity gain that can be utilized by the schedulers. Time division, i.e. allocating the whole band s_2 to one base station for n bin times, in a rotation pattern between the three sites, might on the other hand create problems for traffic classes with tight delay constraints.

reduction due to reuse, and the corresponding reduction of the interference level, in a straightforward way.

Compared to a system with frequency reuse 1 also in the outer part of the cell, the number of usable time-frequency bins will be reduced to a fraction

$$c_2 = \frac{s_1 + (1/3)s_2}{s_0} \ . \tag{2}$$

Assume here a triangular sector, see Figure 2. The geometry and reasoning for diamond-shaped sectors becomes identical, due to symmetry: The lower half of the triangular sector corresponds to the upper half of the diamond-shaped sector. From the geometry, with 60^o sectors with side R,

$$\frac{R/2}{d} = \tan 30^o \ \Rightarrow \ d = \frac{1}{2\tan 30^o} R = \cos 30^o R \ \approx \ 0.86603R \ , \tag{3}$$

or $R = 2(\tan 30^o)d \approx 1.1547d$. The total area A of the sector, the area A_1 of the inner zone 1 and the area A_2 of the outer zone 2 are

$$\begin{aligned} A &= d\frac{R}{2} = d^2 \tan 30^o \ = \ 0.57735\, d^2 & (4)\\ A_1 &= d_1^2 \tan 30^o & (5)\\ A_2 &= A - A_1 = (d^2 - d_1^2)\tan 30^o \ . & (6) \end{aligned}$$

Assuming constant user density per unit area, we partition the total spectral band s_0 in proportion to the areas of the two zones:

$$\begin{aligned} \frac{s_1}{s_0} &= \frac{A_1}{A} = \left(\frac{d_1}{d}\right)^2 & (7)\\ \frac{s_2}{s_0} &= \frac{A_2}{A} = 1 - \left(\frac{d_1}{d}\right)^2 \ . & (8) \end{aligned}$$

This resource partitioning depends only on the distance limit d_1 and not on the sector width (for sector angles $< 180^o$). It can thus be used over the whole system, also if other sites have other numbers of sectors, or if the beam-widths and angles are adjusted adaptively.[4]

The use of (7)(8) in (2), combined with (1), gives the following expression for the fraction of usable time-frequency bins, after the reductions due to the reuse pattern in zone 2 and the coordinated scheduling of border users:

$$c_{\text{tot}} = c_1 c_2 = \left(1 - \frac{\beta}{60^o}\right)\left(\left(\frac{d_1}{d}\right)^2 + \frac{1}{3}\left(1 - \left(\frac{d_1}{d}\right)^2\right)\right) \ . \tag{9}$$

For example, for $d_1^2/d^2 = 0.5$, we obtain $c_{\text{tot}} = (7/8)(2/3) = 7/12$, which corresponds to an *equivalent reuse factor* of $1/c_{\text{tot}} \approx 1.71$. Our general aim is to obtain a good interference suppression, while, if possible, not having to use an equivalent reuse factor above 2.

[4]With unequal traffic distribution within the cell, the partitioning should be with respect to *traffic demand* rather than *area*. Note that we here assume the fractions s_1/s_0 and s_2/s_0 to be equal in all cells. The consequences of unequal partitioning due to unequal demand is a topic for future research.

5 The SIR due to Path Loss and Interference

We now calculate the interference generated by all base stations of significance. All interferers within a distance $5.5R$ from some part of the sector of interest are taken into account. Short-term frequency selective fading and log-normal shadow fading are here neglected. Only the path loss is taken into account, and it is assumed to follow a simple power law (the Okamura-Hata model)

$$P_R = \frac{g}{r^\alpha} P_T \ , \tag{10}$$

where P_R is the received power. The factor g depends on the heights transmit and receive antennas and on the carrier frequency. It is here assumed to be a constant for all transmitter-receiver pairs and it will then cancel in the evaluation below.

Furthermore, P_T is the transmitted power and r is the distance between the transmitter and the receiver. The attenuation exponent α is a variable, for which the default value $\alpha = 4$ will be used below.[5] The SIR encountered by a user located at (x, y) in the inner zone 1 of our sector of interest will be

$$\text{SIR} = \frac{\frac{g}{r^\alpha} P(\theta)}{\ell(\sum_i \frac{g}{r_i^\alpha} P(\varphi) + g I_s(\theta))} \ , \tag{11}$$

where i is a sum over all interferers indicated in Figure 1. Here,

$r = \sqrt{x^2 + y^2}$ is the distance from the user to the base station.[6]

$\theta = \arctan(x/y)$ is the angle to the user, relative to the sector symmetry line.

$P(\theta)$ is the angle-dependent antenna pattern that is illustrated by Figure 3. (Note that power is boosted by 2 when $\theta > 30^o - \beta$ and $\theta < -30^o + \beta$.)

ℓ is the traffic load factor in interfering cells. It affects the interference level.

$P(\varphi)$ is the transmit power of the interfering antenna at angle φ.
Its average is $\mathrm{E}_\varphi[P(\varphi)] = 0.847 P(0)$, or $P(0)_{dB} - 0.76$ dB.

$r_i = \sqrt{(x - x_i)^2 + (y - y_i)^2}$ is the distance to interferer i, located at (x_i, y_i).

$I_s(\theta)$ is remaining power due to interference from adjacent sectors at the site,

[5]For free space transmission, $\alpha = 2$, which will hold only very close to the base station. Farther away, we have ground reflex effects which result in approximately $\alpha = 4$, see e.g. [6]. Multipath propagation in outdoor environments complicates the picture, but a value of α somewhat above 4 seems reasonable for cells up to 10km, carrier frequencies around 2 GHz, transmit antenna heights of 20-50 m and receiver antenna heights below 10m, for rural and suburban environments [7]. Some measurements have tended to find exponents closer to 3 than to 4. For propagation over heavily forested areas, we may have α as high as 6 (see e.g. Section 4.4 of [8]).

[6]The calculations are independent of the absolute scales of r (in meters) and P (in Watts) since we assume an interference-limited scenario. The absolute scales would matter if a noise term were included in the denominator of (11).

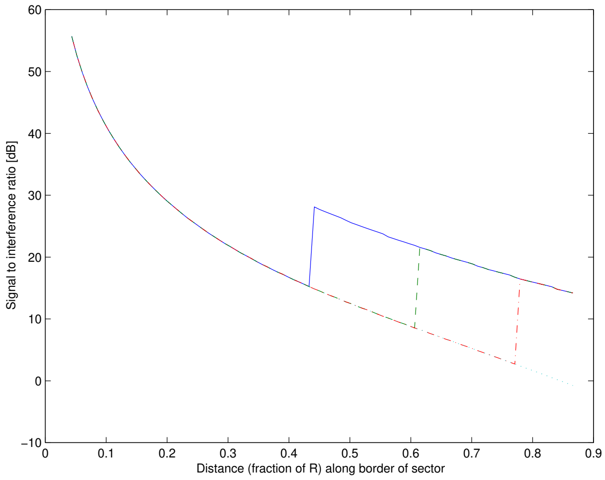

Figure 4: The SIR in dB along the *center* of the triangular sector, as a function of the distance from the base station, measured in units of the triangle side length R. The border between zone 1 and zone 2, d_1, is $0.50d$ (solid), $0.71d$ (dashed) and $0.90d$ (dash-dotted). The lower outer dotted curve corresponds to $d_1 = d$, i.e frequency reuse one out to the border of the sector. The traffic load is $\ell = 1$ and the propagation exponent is $\alpha = 4$.

for $-30^o + \beta < \theta < 30^o - \beta$. (See Figure 3.)

The traffic load factor $\ell = 1$ and the propagation exponent $\alpha = 4$ are used in the following, unless stated otherwise.

In the outer zone 2 of the sector, the expression for the SIR is similar to (11), except that we there only have to sum over the active cell sites within the neighboring 3-site clusters. As indicated by Figure 1, there are 12 such sites within the distance $5.5R$ from our sector, denoted by stars within the rings. We have six interferers at distance $\approx 3R$ and six at distance $\approx 5R$.

To give an example, we may thus, for $\alpha = 4$ and $\ell = 1$, expect a SIR of approximately

$$\begin{aligned} \text{SIR}(d, 0.5R) &\approx \frac{\frac{1}{R^\alpha}P(30^o)}{\left(6\frac{1}{3R^\alpha} + 6\frac{1}{5R^\alpha}\right)0.847P(0^o)} = \frac{1}{\left(\frac{1}{81} + \frac{1}{625}\right)5.08}10^{(-8+3)/10} \\ &\approx 14.11 \times 0.316 = 4.46 \approx 6.5 \text{ dB} \end{aligned} \quad (12)$$

for a user located at the outer corner $x = d,\ y = R/2$ of the triangular sector, at distance R. An average has here been taken over the angles to the interferers, with $\mathrm{E}_\varphi[P(\varphi)] = 0.847P(0)$. The factor $P(30^o)/P(0^o) = 10^{(-8+3)/10}$ is due to the 8 dB damping of the antenna pattern at 30^o, partly compensated by the 3 dB power boost at these angles, see Section 3.

Figure 4 shows the SIR calculated by (11) along the center of the triangular sector (for $\theta = 0$) from $x = 0.05R$ to $x = d$ for three values of the border distance d_1: $d_1 = 0.50d$ ($A_2 = 0.75A$), $d_1 = 0.71d$ ($A_2 = 0.50A$) and $d_1 = 0.90d$ ($A_2 = 0.19A$). The corresponding equivalent reuse factor $1/c_{\text{tot}}$ according to (9) is then 2.29, 1.71 and 1.36, respectively. Figure 5 shows the SIR along the edge of the

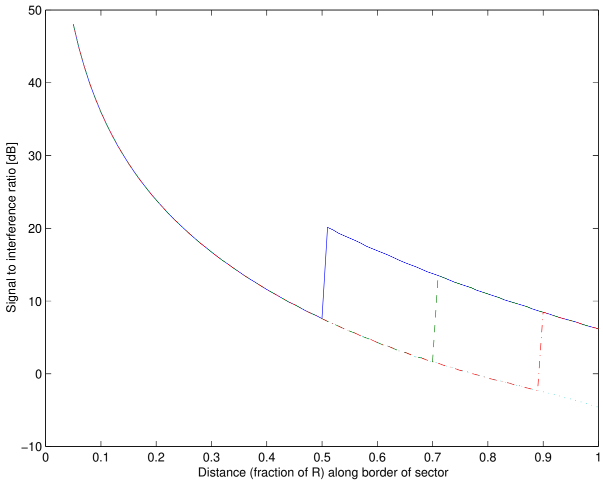

Figure 5: The SIR in dB along the *outer edge* of the triangular sector, as a function of the distance from the base station, measured in units of the triangle side length R. The border between zone 1 and zone 2, d_1, is $0.50d$ (solid), $0.71d$ (dashed) and $0.90d$ (dash-dotted). The lower outer dotted curve corresponds to $d_1 = d$, i.e frequency reuse one out to the border of the sector. The traffic load factor is $\ell = 1$ and $\alpha = 4$.

sector, at angle $\theta = 30^o$. The SIR at the outer corner, at distance $1.0R$, is 6.2 dB, so the approximations used in (12) turned out to be rather accurate.

We may in Figure 4 and Figure 5 note the following:

- The SIR improves by 12dB when entering zone 2 from zone 1. If we would expand zone 1 to the outer cell boundary (dotted line), interference would make transmission impossible with our rate boundaries for adaptive modulation beyond $d = 0.7R$, where the SIR would be 5.5 dB in the center of the sector (Figure 4). Without a zone 2, the SIR would in the outer areas along the outer edge (Figure 5) have been below 0dB. The transmission quality variations are also reduced. For example, we may obtain a SIR $\approx$ 12 dB in the distance range $d > 0.45R$ in Figure 4 if we select $d_1 = 0.71d = 0.61R$.
- The choice of d_1 does not affect the SIR levels encountered within zone 2. That is because the interference power will be independent of the choice of d_1 in the interfering cells: If the area A_2 is increased, the frequency allocation s_2 will be increased in the same proportion, cf. (8). The interference power per unit frequency will therefore remain constant.
- The SIR will be rather low close to the sector edge in the outer part of zone 1 (for d somewhat lower than d_1) in the triangular sector. The worst SIR is for $d_1 \geq 0.55d$ encountered in the outer part of zone 1 at high angles θ.
- The assumed shape of the zone boundary is better adjusted to the beam pattern in the diamond-shaped sector than in the triangular sector.

Figures 6-7 show color contour plots of the SIR distribution within the sectors for $d_1 = 0.60d = 0.52R,\ d_1 = 0.70d = 0.61R$ and $d_1 = 0.90d = 0.779R$.

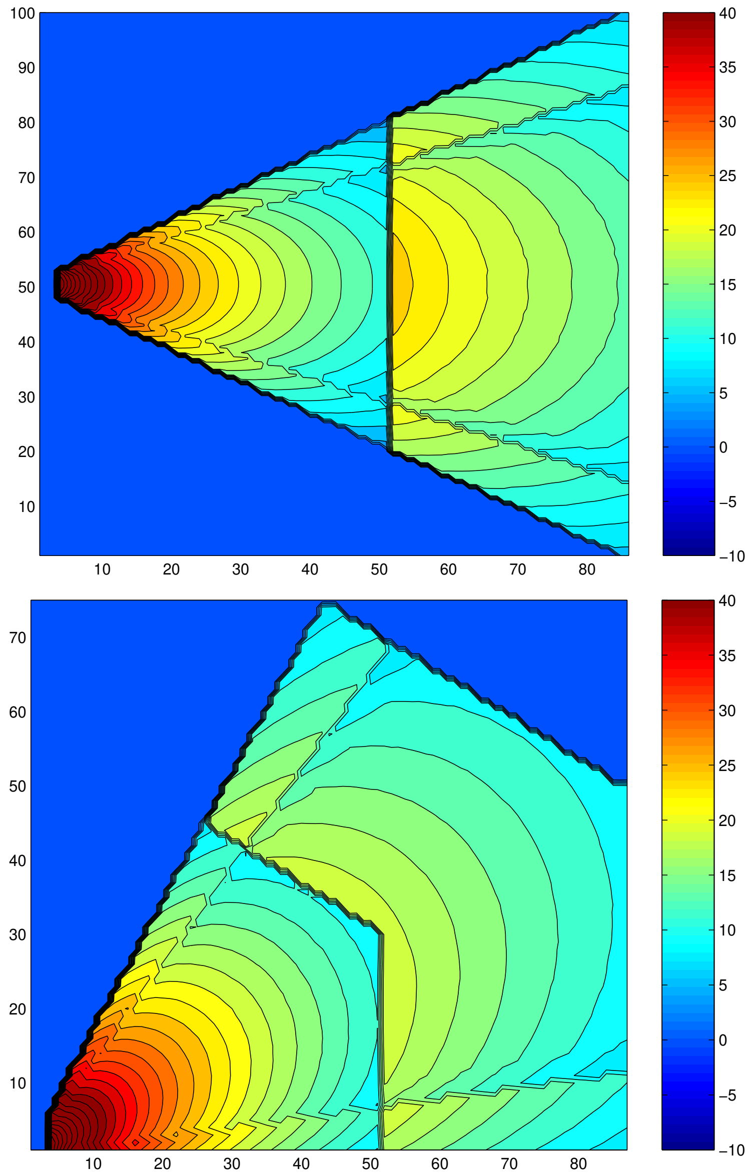

Figure 6: Distribution of the SIR in dB for $d_1 = 0.60d = 0.52R$. within the triangular sector (upper figure) and the diamond-shaped sector (lower figure). The traffic load factor is $\ell = 1$ and the propagation exponent is $\alpha = 4$.

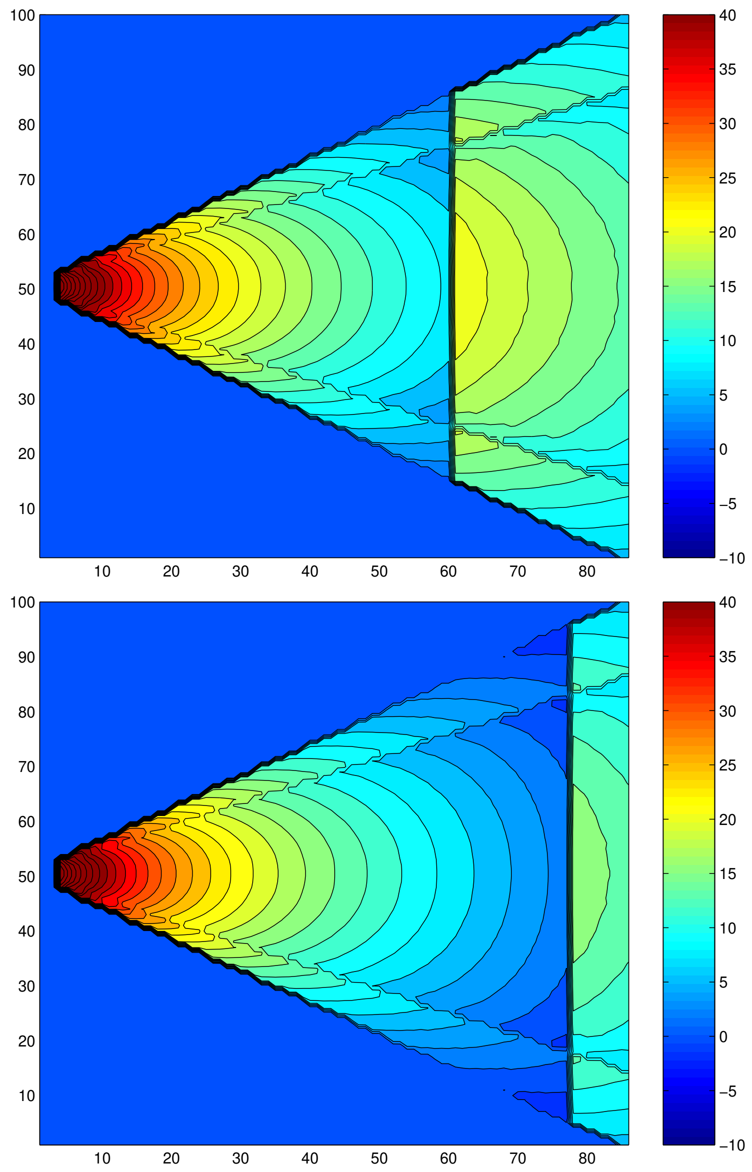

Figure 7: Distribution of the SIR in dB within the triangular sector for $d_1 = 0.70d = 0.61R$ (upper figure) and $d_1 = 0.90d = 0.78R$ (lower figure). The traffic load factor is $\ell = 1$ and the propagation exponent is $\alpha = 4$.

6 Deterministic Estimate of the Spectral Efficiency

We now estimate the raw spectral efficiency (the number of bits per symbol) when using uncoded adaptive modulation. In this section, the effects of path loss are taken into account via (11), while Rayleigh short-term fading will be added in Sections 8 and 9. For a given instantaneous SIR (symbol energy relative to interference energy) γ_t, we consider the average *goodput* defined by

$$g(\gamma_t, k_i) \stackrel{\Delta}{=} P_p(\gamma_t, k_i)k_i \quad \text{[bits/symbol]} \tag{13}$$

where k_i is the number of bits/symbol in the utilized modulation format and $P_p(\gamma_t, k_i)$ is the probability that the link level packet (frame) will be delivered correctly. This probability is given by

$$P_p(\gamma_t, k_i) = (1 - P_s(\gamma_t, k_i))^F \ \ , \ \ P_E = 1 - P_p(\gamma_t, k_i) \tag{14}$$

where $P_s(\gamma_t, k_i)$ is the symbol error rate and F is the frame size, the number of payload symbols per link level packet. Thus, the link level packet error rate is $P_E = 1 - P_p$. In our adaptive OFDM system, there are 120 symbols per bin, of which 108 are payload symbols. Thus, $F = 108$ will be assumed. The quantity gF will always correspond to the steady-state througput rate of correct bits per frame duration. (The number of dropped packets will depend on the maximum allowed number of link level retransmissions.)

If we assume the interference to be Gaussian, and that BPSK or M-QAM is used, the symbol error rate will, for $M = 2^{k_i}$ be given by ([9], Chapter 4)

$$P_s \;=\; \begin{cases} 0.5\,\mathrm{erfc}(\sqrt{\gamma_t}) & k_i = 1 \quad \text{(BPSK)} \\ 1 - \left[1 - \left(1 - \frac{1}{\sqrt{M}}\right)\,\mathrm{erfc}\left(\sqrt{\frac{3\gamma_t}{2(M-1)}}\,\right)\right]^2 & k_i = 2, 4, 6, 8 \ldots \\ 1 - \left[1 - \mathrm{erfc}\left(\sqrt{\frac{3\gamma_t}{2(M-1)}}\,\right)\right]^2 & k_i = 3, 5, 7 \ldots \ . \end{cases} \tag{15}$$

The first and second expressions are exact, while the third is a tight upper bound. In our adaptive OFDM system, we assume the use of $k_i \leq 8$ and of cross-QAM constellations for $k_i = 3, 5$ and 7.

The *rate limits* γ_i, i.e. the SIR thresholds for use of rate k_i, can be optimized by using (15). In [2], we adjusted them to attain $P_E = 10\%$ packet error rate at the thresholds. Better overall performance was attained in [3] by adjusting the thresholds to obtain an *average* packet error rate $\mathrm{E}\,(P_E) = 10\%$ for a Rayleigh fading channel at 16 dB average SINR. The corresponding rate limits are given in the middle part of Table 1 below. However, since we do *not* have an SIR of 16 dB everywhere within the sector, we cannot guarantee that an adaptive modulation level tuned in this way will in fact satisfy the average symbol error rate constraint.

Here, we will instead remove all packet error rate constraints, and directly optimize the goodput (13). A rate limit is then characterized by the property that the gain obtained with a higher k_i would be exactly balanced by the loss due to a lower P_p:

$$(1 - P_s(\gamma_t, k_i))^F k_i = (1 - P_s(\gamma_t, k_{i+1}))^F k_{i+1} \ . \tag{16}$$

The resulting SIR thresholds are presented in the right-hand part of Table 1. The main difference as compared to the old thresholds is that the lower cutoff SIR bound k_0 for using BPSK has been removed. (It is better to get something than nothing.) The new adjustment will therefore primarily improve the spectral efficiency at low SIRs.[7] In the following, we in practice set this threshold at SIRs such that $P_p = 0.1$. We define *sector coverage* as the percentage of area within the sector where $P_p \geq 0.1$.

i	Modulation	k_i	from [3] γ_i (dB)	New: γ_i (dB)	γ_i
0	BPSK	1	5.5	$-\infty$	0
1	4-QAM	2	8.7	8.70	7.42
2	cross-8-QAM	3	13.4	13.53	22.55
3	16-QAM	4	16.6	16.88	48.8
4	cross-32-QAM	5	20.3	20.46	111.2
5	64-QAM	6	23.5	23.39	228.7
6	cross-128-QAM	7	26.9	26.86	484.7
7	256-QAM	8	30.0	29.94	985.7

Table 1: Optimized switching levels γ_i in dB, for the lowest SINR per symbol and receiver antenna for using modulation with k_i bits per symbol. The limits in the center are adjusted for an average symbol error rate 9.8×10^{-4} for users with Rayleigh fading channels at 16 dB SINR. Right-hand limits maximize the goodput defined by (13).

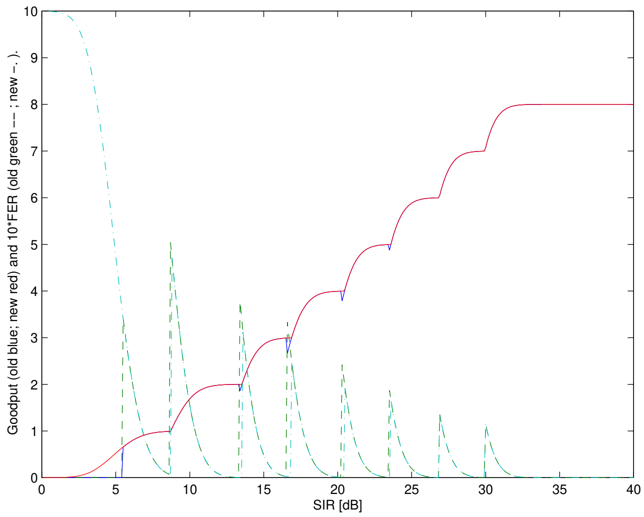

Figure 8: The goodput g as a function of the instantaneous SIR γ_t in dB, when using the old (blue) and the new (red) rate limits. It also illustrates the resulting packet error rate, multiplied by 10, for $F = 108$. The dashed curve is for the old limits while the dash-dotted is for the new.

Figure 8 displays the goodput g as a function of the instantaneous SIR γ_t, when using the old and the new rate limits. It also illustrates the packet error rate.

[7] In practice, one *should* of course utilize a lower threshold, since a user will create interference. The adjustment of this threshold should however be performed from a system capacity perspective and not, as is common in the literature on adaptive modulation, from a BER constraint. This adjustment represents still another sub-problem for research.

An estimate can now be obtained for the capacity in bit/s/Hz as a function of the position within the sector. This value should be interpreted as representing the following situation

- The user is alone in the sector, and is not moving, with a constant channel gain that is independent of frequency. We thus do not take multiuser diversity effects into account here, and do not utilize the variability of the channel in time and frequency. The situation is somewhat related to that of $K = 1$ user with $L = 1$ receiver antenna in [2] and [3], where the channel was assumed Rayleigh fading. In the present and the next chapter, the channel is assumed static, while Rayleigh and Rice fading is introduced in Sections 8 and 9.
- The number of bits per symbols obtained in the outer zone 2 will of course have to be multiplied by $1/3$ to obtain the spectral efficiency for the frequency region s_2.
- In both zones, we have to multiply by the factor $c_1 = 7/8$ by (1) to take the capacity loss due to scheduling between sectors into account.

Figure 9 shows the so calculated spectral efficiency within the triangular sector for the two values $d_1 = 0.50d = 0.433R$ and $d_1 = 0.71d = 0.61R$ for the border between zone 1 and zone 2.

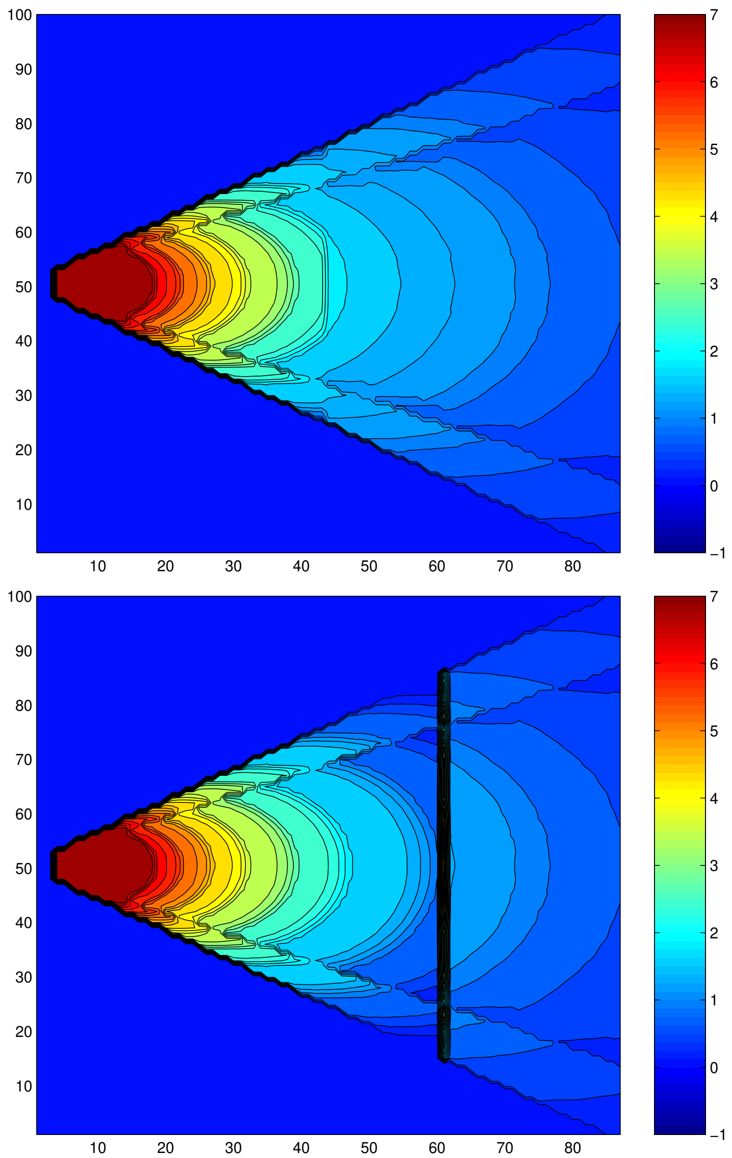

Figure 9: Raw spectral efficiency in bit/s/Hz as a function of the position within the triangular sector for $d_1 = 0.50d = 0.433R$ (upper figure) and $d_1 = 0.71d = 0.61R$ (lower figure). The traffic load factor is $\ell = 1$ and the propagation exponent is $\alpha = 4$.

7 Optimization of Zone Border (Deterministic Case)

The zone boundary d_1 is the main system parameter. For $d_1 = 0$ we would have a reuse 3 system, while $d_1 = 1$ would result is a system with frequency reuse 1. There seems to be an optimal value in-between. The main criterion to optimize would be the *average spectral efficiency within the sector* $\bar{\eta}$, which is given by

$$\bar{\eta} \triangleq \frac{\eta_1 s_1 + \eta_2 s_2}{s_0} = c_1 \left(\bar{g}_{i1} \frac{A_1}{A} + \frac{1}{3} \bar{g}_{i2} \frac{A_2}{A} \right) \text{ [bit/s/Hz]} . \tag{17}$$

Here, η_1 and η_2 are the average spectral efficiencies within zone 1 and zone 2, respectively, while $\bar{g}_{i1}$ and $\bar{g}_{i2}$ are the averages over the areas of zone 1 and zone 2 of the goodput (bits per symbol weighted by packet acceptance rate) according to (13). New rate limits in Table 1 are used. The factor $c_1 = 7/8$ is from (1).

Another factor that should be taken into account is the *sector coverage* which we have, somewhat arbitrarily, defined as the fraction of the area where the goodput is above 0.1 bits/symbol.[8] Ideally, we would like to find a value of d_1 that both attains a high spectral efficiency and assures a good coverage. These and other properties are investigated in Table 2 for the triangular sector and in Table 3 for the diamond-shaped sector, by varying d_1 from 0 to 1 in steps of 0.1. The estimates are for a fully loaded system $\ell = 1$, which is appropriate in an estimation of the system capacity. A more realistic case of $\ell = 0.25$ reduces the interference level by 6 dB, compared to the fully loaded case. Results are shown for that case in the last line of the tables, for $d_1 = 0.6$. Figure 10 illustrates some of the results.

d_1/d	d_1/R	η_1	η_2	$\bar{\eta}$	% Sector coverage	% ≥ 16 QAM	Reuse $1/c_{\text{tot}}$	Average SIR [dB]	Average FER %
0.0	0	(0)	1.27	**1.27**	**100**	60	3.42	19.5	5.2
0.1	0.087	7	1.26	**1.31**	**100**	60	3.36	19.4	5.2
0.2	0.173	6.79	1.22	**1.44**	**100**	60	3.17	19.1	5.3
0.3	0.260	5.94	1.15	**1.59**	**100**	60	2.90	18.6	5.4
0.4	0.346	4.76	1.07	**1.66**	**100**	59	2.60	17.9	5.7
0.5	0.433	3.85	0.97	**1.69**	**100**	51	2.29	16.9	6.1
0.6	0.520	3.22	0.87	**1.72**	**100**	41	1.99	15.9	6.8
0.7	0.610	2.59	0.77	**1.67**	**100**	29	1.73	14.4	9.1
0.8	0.693	2.05	0.69	**1.56**	**96**	20	1.50	12.7	13.3
0.9	0.779	1.68	0.60	**1.47**	**86**	16	1.36	10.8	17.6
1.0	0.866	1.35	(0)	**1.36**	**67**	16	1.14	8.4	20.5
(0.6	0.520	4.56	1.38	**2.52**	**100**	87	1.99	21.9	4.1)

Table 2: The average spectral efficiency η_1 in the inner zone 1 and η_1 in the outer zone 2, and the total average spectral efficiency $\bar{\eta}$ bit/s/Hz, as a function of the zone boundary d_1, for the **triangular sector**. Also shown is the fraction of area with coverage and the fraction of area where 16QAM or higher modulation levels can be used, as well as the average SIR, the equivalent reuse $1/c_{\text{tot}}$ by (9) and P_E by (14). Last line is for traffic load $\ell = 0.25$ while the all other values are for $\ell = 1$. The path loss is $\alpha = 4$.

[8]Note, however, that shadow fading has been neglected in this simplified discussion. Shadowing would in practice always result in spots without coverage.

d_1/d	d_1/R	η_1	η_2	$\bar{\eta}$	% Sector coverage	% ≥ 16 QAM	Reuse $1/c_{\text{tot}}$	Average SIR [dB]	Average FER %
0.0	0	(0)	1.11	**1.11**	**100**	48	3.42	19.1	5.1
0.1	0.087	7	1.10	**1.16**	**100**	48	3.36	19.1	5.1
0.2	0.173	7	1.06	**1.30**	**100**	48	3.17	18.9	5.1
0.3	0.260	6.44	0.99	**1.48**	**100**	48	2.90	18.6	5.2
0.4	0.346	5.34	0.91	**1.62**	**100**	48	2.60	18.0	5.3
0.5	0.433	4.38	0.82	**1.71**	**100**	43	2.29	17.3	5.5
0.6	0.520	3.62	0.74	**1.78**	**100**	33	1.99	16.3	5.7
0.7	0.610	2.91	0.64	**1.77**	**100**	21	1.73	15.1	6.9
0.8	0.693	2.31	0.59	**1.69**	**99**	19	1.50	13.4	12.7
0.9	0.779	1.86	0.54	**1.61**	**86**	19	1.36	11.6	15.2
1.0	0.866	1.51	(0)	**1.51**	**69**	19	1.14	9.3	17.8
(0.6	0.520	4.96	1.23	**2.58**	**100**	91	1.99	22.4	4.3)

Table 3: The average spectral efficiency η_1 in the inner zone 1 and η_1 in the outer zone 2, and the total average spectral efficiency $\bar{\eta}$ bit/s/Hz, as a function of the zone boundary d_1, for the **diamond-shaped sector**. Also shown is the fraction of area with coverage and the fraction of area where 16QAM or higher modulation can be used, as well as the average SIR, the equivalent reuse factor $1/c_{\text{tot}}$ by (9) and P_E by (14). Last line is for traffic load $\ell = 0.25$ while the all other values are for $\ell = 1$. The path loss is $\alpha = 4$.

It is evident that a border d_1 around $0.6d - 0.7d$ will both maximize the average spectral efficiency and also assure at least some coverage within the whole sector.

When comparing the results presented in Table 2, Table 3 and Figure 10, one may note the following.

- Both the overall spectral efficiency and the coverage become somewhat better for diamond-shaped sectors as compared to triangular sectors.
- The spectral efficiency η_1 within the inner zone 1 is clearly higher for the diamond-shaped sector. This is because zone 1 is affected by nearby interferers and the diamond geometry shifts the angle of the sectors so that no nearby sectors point directly towards each other. This reduces the interference, due to the assumed antenna pattern of Figure 3: The interference power is reduced by around 5 dB at 30^o angle relative to a situation where the center of a sector of an interfering cell points directly towards us.
- On the other hand, the spectral efficiency η_2 within the outer zone 2 is worse for the diamond-shaped cell than for the triangular cell. The reason is that one of the nearest of the 12 interfering cells that transmit in s_2 (belonging to the site at $x = 2.59R, y = 1.5R$ in Figure 1) will point directly toward the diamond-shaped sector with direction $+30^o$ of the site at $x = 0, y = 0$.

To summarize, diamond-shaped 60^o sectors in hexagonal coverage areas provide a somewhat higher spectral efficiency than triangular sectors, at the price of reducing the already low capacity offered within zone 2. The triangular sector might be preferred for that reason.

A triangular sector with a diamond-shaped zone 1 with the same symmetry axis was also tested, since such a border shape follows the sector beam pattern

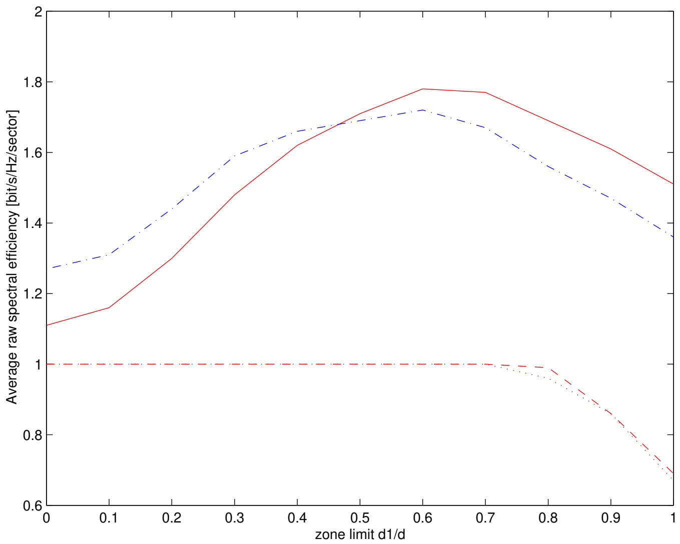

Figure 10: The average spectral efficiency $\bar{\eta}_s$ for a user with time-invariant (static) channel within the diamond sector (solid,red) and the triangular sector (dash-dotted,blue). Also shown is the fraction of area with coverage, (dashed red for the diamond sector, dotted blue for the triangular sector) as a function of the relative position of the zone boundary d_1/d in the 60^o sector. The traffic load factor is $\ell = 1$ and the path loss exponent is $\alpha = 4$.

better. The performance of this design was almost identical to that of the basic triangular sector.

With adaptive base station antennas, one could transmit in diamond-shaped sectors (rotated by 30^o) to nearby users at the frequencies s_1, while triangular sectors are used at frequencies s_2 for contacting the far users. The geometry fits nicely, and the result would be a pattern that inherits the strengths of both designs, but not their weaknesses. The spectral efficiency in zone 1 would be η_1 from Table 3 while we in zone 2 would have η_2 from Table 2. With a border $d_1 = 0.6d$ this would result in a total average spectral efficiency $\bar{\eta} = 1.86$ bit/s/Hz.

Use of the new rate limits of Table 1 as opposed to the old ones resulted in an improvement of the spectral efficiency by around 4% at $\ell = 1$ and 6% at $\ell = 0.25$.

8 Spectral Efficiency for One Rayleigh Fading User

Several sector designs and a strategy for frequency planning for interference avoidance have been proposed and investigated, but so far only for static path loss channel models. A reasonable framework for a preliminary investigation that takes fading channels, multiuser diversity and multiple receiver antennas into account is outlined below:

- Continue to take only the path loss of the interferers into account. Since the interferers are many, their short term fading and shadow fading will be assumed to average out.
- Complement the path loss model for the received signal with a Rice model for the short-term fading. We continue to neglect the shadow fading at

present. Since the fading of the interference is neglected, the SIR is therefore assumed described by a path loss together with Rice fading. A Rice model has the presently investigated time-invariant channel and the Rayleigh fading channel as its two extreme points.

- In our preliminary theoretical investigation of the spectral efficiency for Rayleigh fading channels in [2, 3], we assumed that all users have the same average SIR. This would be hard to attain, except by extremely wasteful strategies for slow power control. A simple scheduler that works in more realistic settings, with unequal average user capacities, has to be introduced. A possible candidate algorithm is to allocate the time-frequency bin to the user who has data in queue and who has the best channel capacity *relative* to his own average channel capacity. If the *relative* capacity variations have the same statistics for all users, as they will for Rayleigh fading channels with differing average powers, this scheduler will allocate equal time-frequency resources (but not equal bit rates!) to all active users with data to receive.

The strategies above will be utilized in Section 9 below. As a first step in this investigation of fading channels, we will in this chapter investigate the spectral efficiency for a single user who always has data in the queue. The channel is assumed constant within the time-frequency bins and Rayleigh fading between bins. The user equipment may have L antenna branches, and uses Maximum Ratio Combining (MRC).[9] This case corresponds to the case of $K = 1$ user with L antennas in [3].[10]

Assume that the received SIR has average $\bar{\gamma}$, in a linear scale. The instantaneous received power γ_t over a Rayleigh fading channel will then have the distribution [2, 3], [13]:

$$p(\gamma_t|\bar{\gamma}, L) = \frac{1}{\bar{\gamma}} \frac{e^{-\gamma_t/\bar{\gamma}} \left(\gamma_t/\bar{\gamma}\right)^{L-1}}{\Gamma(L)} U(\gamma_t) \ , \tag{18}$$

where $U(\,\cdot\,)$ is Heaviside's step function. For users with a single antenna, $L = 1$, (18) reduces to the exponential distribution

$$p(\gamma_t|\bar{\gamma}, L = 1) = \frac{1}{\bar{\gamma}} e^{-\gamma_t/\bar{\gamma}} U(\gamma_t) \tag{19}$$

for the power of a Rayleigh fading complex channel tap.

When transmitting symbols at the sampling rate (1/bandwidth), the spectral efficiency η_f with adaptive modulation over a fading channel will here be obtained

[9] An assumption of Rayleigh fading and use of MRC corresponds to an assumption of a rich scattering environment close to the mobile. This scattering results in signals and interference arriving isotropically from all azimuth angles around the terminal. Under these conditions, coherent detection and MRC is the receiver algorithm that makes best use of the L receiver branches.

More realistic scenarios would involve a few dominating distant scatterers and some additional close scatterers. The signal of interest and the interferer signals would then arrive from a few angles, with some angular spread. Interference Rejection Combining, IRC (i.e. using the inverse of the interference covariance matrix in the multi-antenna receiver) could then be expected to provide superior performance as compared to MRC. This is an important topic for future research.

[10] As noted in [4], this case also corresponds to the use of a downlink transmitter with L antennas in each sector, that uses ideal downlink beamforming. Such a scheme does, however, require channel information at the transmitter.

by a weighted average of the goodput (13) over the symbol modulation formats, weighted by the probabilities that those particular formats will be utilized

$$\eta_f(\bar{\gamma}, L) = \sum_i k_i \int_{\gamma_i}^{\gamma_{i+1}} P_p(\gamma, k_i) p(\gamma|\bar{\gamma}, L) d\gamma \quad \text{[bit/s/Hz]} \ . \tag{20}$$

Due to the weighting with the packet acceptance probability $P_p(\ \cdot\ )$, η_f will be denoted the *weighted* spectral efficiency of the adaptive modulation scheme over a flat fading channel. This function has been evaluated by numerical integration for $L = 1, L = 2$ and $L = 4$, using the new rate limits γ_i of Table 1. The result is shown in Figure 11 below. With $k_i \in [\ 1\ 2\ 3\ 4\ 5\ 6\ 7\ 8\ ]$, η_f saturates at 8 at high SIR. As expected, we gain 3 dB when going from $L = 1$ to $L = 2$, and another 3 dB when increasing L from 2 to 4. The goodput (13), displayed in Figure 8, has a "soft staircase" form, which is not present in the function η_f.

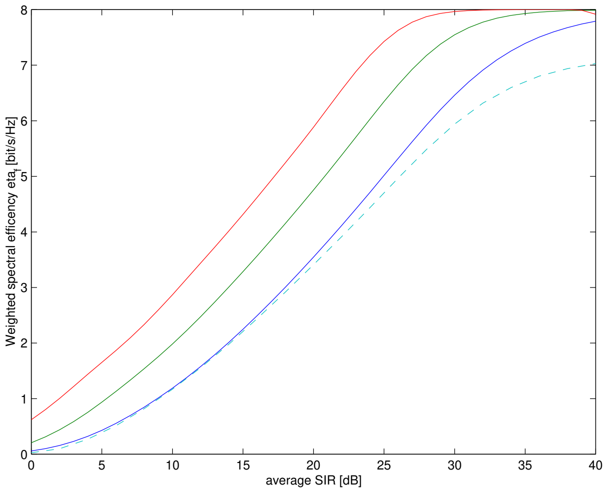

Figure 11: The weighted spectral efficiency η_f by (20) as a function of the SIR $\bar{\gamma}$ for a user who applies MRC with $L = 1$ (lowest), $L = 2$ (middle) and $L = 4$ (upper) receiver antennas. Also shown is the estimated η_f when using the old rate limits of [3] (dashed).

As a comparison, the dashed line shows an estimate for $L = 1$ obtained with the old rate limits of Table 1, under the assumption of a 10% average link level packet (frame) error rate (FER).[11] The difference at high SIR between the old and new schemes is mainly due to that the frame error rate is significantly below 10% in these regions, while we assume a 10% loss in the dashed curve.

[11]This estimate is obtained by substituting $P_p(\gamma, k_i)$ in (20) by its assumed average value 0.9 everywhere, and thus removing it outside of the integration. For (19), we have

$$\int_{\gamma_i}^{\gamma_{i+1}} p(\gamma) d\gamma = \frac{1}{\bar{\gamma}} \int_{\gamma_i}^{\gamma_{i+1}} e^{-\gamma/\bar{\gamma}} d\gamma = \left[-e^{-\gamma/\bar{\gamma}} \right]_{\gamma_i}^{\gamma_{i+1}} = e^{-\gamma_i/\bar{\gamma}} - e^{-\gamma_{i+1}/\bar{\gamma}} \ .$$

The use of our modulation formats with $k_i \in [\ 1\ 2\ 3\ 4\ 5\ 6\ 7\ 8\ ]$ and of the above expression in (20) then gives

$$\eta_f(\bar{\gamma}, 1) = 0.9 \sum_{i=0}^{7} e^{-\gamma_i/\bar{\gamma}} \ .$$

With a tabulated $\eta_f(\bar{\gamma}, L)$, it becomes straightforward to investigate the spectral efficiency for a mobile user with Rayleigh fading channel with an average SIR $\bar{\gamma}$, that depends on the position within the sector. The spectral efficiency for a Rayleigh fading channel becomes somewhat lower than for a static channel with SIR $\bar{\gamma}$. Its average $\bar{\eta}_f$ over the sector is shown as a function of the zone border d_1 in Figure 12. For a fully loaded system ($\ell = 1$), the optimum of the limit d_1 changes little with respect to the static case of Figure 10. For $d_1 = 0.6d$, we attain the maximum of $\bar{\eta}_f = 1.525$ for diamond-shaped sectors and $\bar{\eta}_f = 1.47$ for triangular sectors. For sectors with diamond-shaped zone 1 rotated by 30^o and triangular zone 2 (differing beam patterns at the frequencies s_1 and s_2), $\bar{\eta}_f = 1.60$ could be attained.

An assumption of full load, $\ell = 1$, is rather extreme, and is appropriate only for estimating the ultimate total system capacity. Let us investigate the sector capacity in a more benign (and realistic) case, where the load factor is $\ell = 0.25$ and each terminal has $L = 2$ receiver branches, using MRC. We then attain the maximum of $\bar{\eta}_f = 3.01$ for diamond-shaped sectors and $\bar{\eta}_f = 2.89$ for triangular sectors. The result, displayed by the upper curves of Figure 12, shows that the optimal zone boundary is then shifted markedly outward, to around $d_1 = 0.9d$.

The inner zone 1 should thus comprise the major area of sectors in a realistic interference scenario.

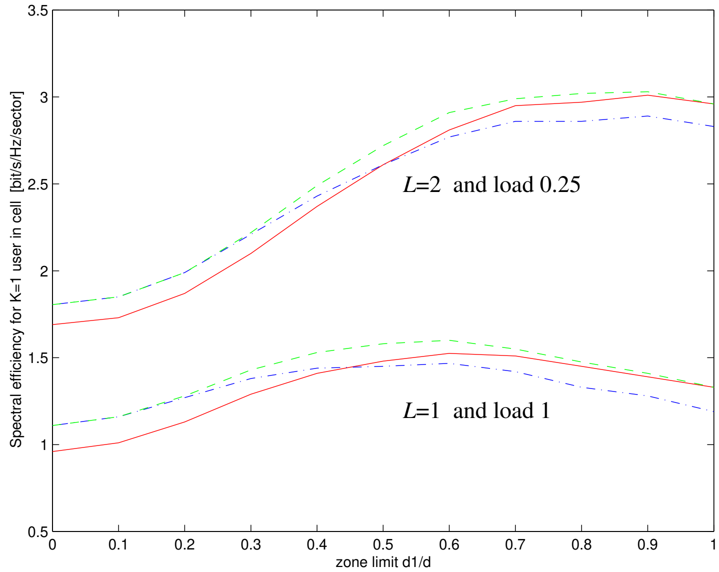

Figure 12: The average spectral efficiency $\bar{\eta}_f$ for one user with Rayleigh fading channel, for the diamond sector (solid,red) and the triangular sector (dash-dotted,blue), as functions of the relative position of the zone boundary d_1/d in the 60^o sector. Also shown is the performance of a beamformer which provides a diamond-shaped zone 1 in the $+30^o$ direction and a triangular zone 2 in the 0^o direction (dashed, green). The lower three curves are for traffic load factor is $\ell = 1$ and $L = 1$ while the upper curves are for $\ell = 0.25$ and $L = 2$ receiver antennas. The path loss exponent is $\alpha = 4$.

9 Average Sector Capacity for K Users with L Antennas, Path Loss and Rice Fading

All tools are now ready to investigate the situation that was considered in the preliminary case studies [2, 3]. In those studies, K active users were assumed to have equal average SIR. Here, they will be randomly distributed within the sector, and an average will be computed over N such situations. Let us summarize the assumptions:

- Flat AWGN channels that are time-invariant within bins and independent Rice fading between bins.
- K active users are present within the cell, at random locations. We consider N one-bin snapshots of such situations, and thus neglect the movement of terminals.
- Accurate SINR predictions, and accurate channel estimation used for symbol detection.
- The target service is reliable packet transmission, while delay constraints are neglected.[12] All users do always have data to transmit, and the allocated bins are fully utilized by their designated users.
- The interference is assume to be isotropic, due to close scatterers. All terminals have L antennas and use MRC.

The complex channel to antenna i of a terminal has been generated as

$$h_i = h_{i0} + \Delta h_i \tag{21}$$

where h_{i0} is constant over bins. It represents a dominating signal path, while Δh_i, a complex Gaussian variable with zero mean, models short-term fading due to numerous close scatterers and reflectors. The variance of Δh_i has been normalized so that h_i has unit second order moment $\mathrm{E}\,|h_i|^2 = 1$:

$$\mathrm{E}\,|\Delta h_i|^2 = 1 - \mathrm{E}\,|h_{i0}|^2 \quad .$$

Deterministic channels are obtained with $\mathrm{E}\,|h_{i0}|^2 = 1$, while pure Rayleigh fading is obtained for $h_{i0} = 0$. If the receiver number j performs Maximum Ratio Combining based on perfect estimates of the channel gains (21), the resulting SIR after MRC becomes[13]

$$\gamma_{t,j} = \frac{P_j}{\sigma^2_{v,j}} \left(\sum_{i=1}^{L} |h_i|^2 \right) \tag{22}$$

[12]The N one-bin snapshots may represent bins separated by time, by frequency or both. For the effectiveness of multiuser diversity for best-effort traffic, it does not matter if the channel variability is in time or in frequency. For traffic classes with delay constraints, such aspects *do* however become important. Flat fading in time over the whole bandwidth will create throughput and delay variations for a user on the timescale of the fast fading. Even worse, for stationary users, the channels may then contain no sub-bands with high gains for extended periods of time. Thus, a sufficiently rich scattering environment which creates frequency selectivity will be important for delay-sensitive traffic. A quantification of this suggestion is yet another topic for research.

[13]See e.g [4], Section 3 on transmit antenna beamforming. MRC in a L-antenna receiver corresponds to optimized beamforming using L transmitter antennas in isotropic noise, and the power gain is the same.

The path loss to a terminal j at a particular location is taken into account by normalizing the transmit power to noise ratio $P_j/\sigma^2_{v,j}$ to the SIR $\bar{\gamma}_j$ that would have been obtained with only one antenna without fading. The average received SIR with MRC among L antennas will thus become

$$\mathrm{E}\left(\gamma_{t,j}\right) = \bar{\gamma}_j L \quad [\mathrm{dB}] \ .$$

As mentioned in Section 8, a method has to be proposed for selecting which of the K users will be allowed to use the bin. In the present study, the necessary quantization of feedback information is neglected. The investigated scheduler selects the terminal for which

$$10 \log_{10}(\gamma_{t,j}) - 10 \log_{10}(\bar{\gamma}_j L) \ \ , \ \ j = 1, \ldots, K \tag{23}$$

is maximized. The scheduler picks the terminal with the best SIR *relative* to his average SIR, measured on a dB scale.

The goodput (13) can now be evaluated via a Monte Carlo simulation, and this has been done as follows. At each of $N = 10000$ runs, K active users are placed randomly within the sector. For each of them, the average SIR $\bar{\gamma}_j$ at that location is computed via (11). The path loss exponent $\alpha = 4$ and the load factor $\ell = 1$ has been used in the investigations below. Random channel taps to the L antennas are then generated by (21), and the resulting instantaneous SIR $\gamma_{t,j}$ is obtained from (22). One of the K users is thereafter selected based on the criterion (23). The instantaneous SIR of that user is used in (13)-(15), which determine the resulting average goodput $\bar{\eta}_f$. This estimate takes the loss of capacity due to frequency reuse and overhead due to packet retransmissions into account. In our adaptive OFDM system, we have a further overhead factor 108/120 due to the 12 pilots and downlink control symbols among the 120 symbols per bin, and 100/111 due to the 11μs cyclical prefix for the 100μs OFDM symbols, see [3]. The product of these factors is 0.811. Taking it into account, and averaging over the N runs results in an estimate of the *sector payload capacity*

$$C_{KLf} = 0.811 \bar{\eta}_f \quad [\text{bit/s/Hz/sector}]$$

with K active users having L antennas in a short-term fading environment.

Preliminary runs with $K = 1$ and $L = 1, 2, 4$ for Rayleigh fading channels ($h_{i0} = 0$) confirmed that Monte-Carlo simulation provides results that correspond closely to the theoretical results of Section 8, when $N \geq 10000$.

The properties of scheduling according to (23) were then investigated. It turns out that the users who are selected are evenly distributed within the cell. Figure 13 shows an example, the distribution of the location of $N = 10000$ selected users when $K = 10$ and $L = 4$. Neither locations with high average SIR nor with low average SIR seem to be preferred. This seems to be a rather desirable property. Users with equal priority are allocated equal time, but their throughput per bin will of course depend on their location. A very marked preference towards regions with extreme average SIR would create problems with bottlenecks and fairness.

The reason for this phenomenon is that the PDFs (18) and (19) of the powers of Rayleigh fading channels has the property that the *relative* channel variability (in dB) is independent of the average power $\bar{\gamma}$, and thus of the location.

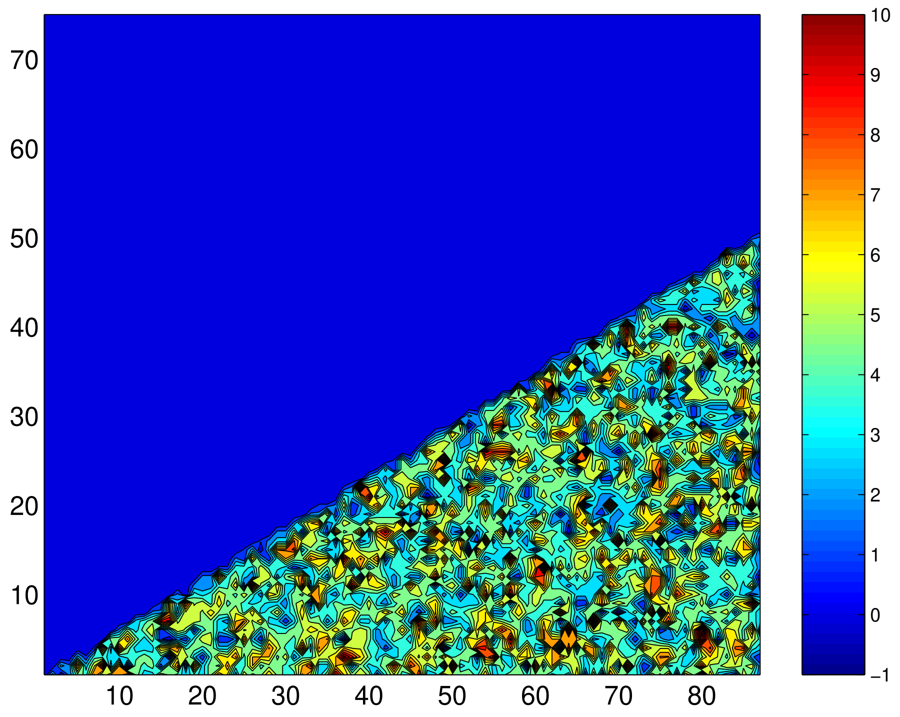

Figure 13: The locations within the lower half of a diamond-shaped sector of 10000 users that were selected by the criterion (23) among $K = 10$ active users, who all had $L = 4$ receiver antennas. The sector boundary was $d_1 = 0.7d = 0.61R$.

Figure 14 shows the resulting sector payload capacity C_{KLf}. The qualitative shape of the curves, and the effect of multiuser diversity, is very similar to that of [2, 3], where equal average SIR 16 dB was assumed for all users. It should be noted that the capacity figures include an equivalent reuse factor (9), which for selected sector boundary $d_1 = 0.7d = 0.61R$ is $1/c_{\text{tot}} \approx 1.73$. If this reuse factor were removed, Figure 14 would look very similar to the corresponding figure in [3], calculated at 16 dB. In fact, as is evident from Table 2 and Table 3, the average over the sector of the SIR turns out to be close to 16 dB when d_1 is selected to be around $0.6d$. We were lucky with our choice of operating point in [3, 2] !

10 Summary of Sector Capacity Results

With the proposed scheme for interference avoidance and the optimized choice $d_1 = 0.6d$ for the zone boundary within diamond-shaped cells, we in Section 7 attained an average raw spectral efficiency for users with *static* (non-fading) channels of

$$\bar{\eta}_s = 1.78 \qquad \text{[bit/s/Hz/sector]} \ .$$

This estimate takes the overhead due to packet retransmissions into account. Taking the additional overhead due to training symbols, control symbols and cyclic prefix into account will in our proposed OFDM downlink result in the sector pay-

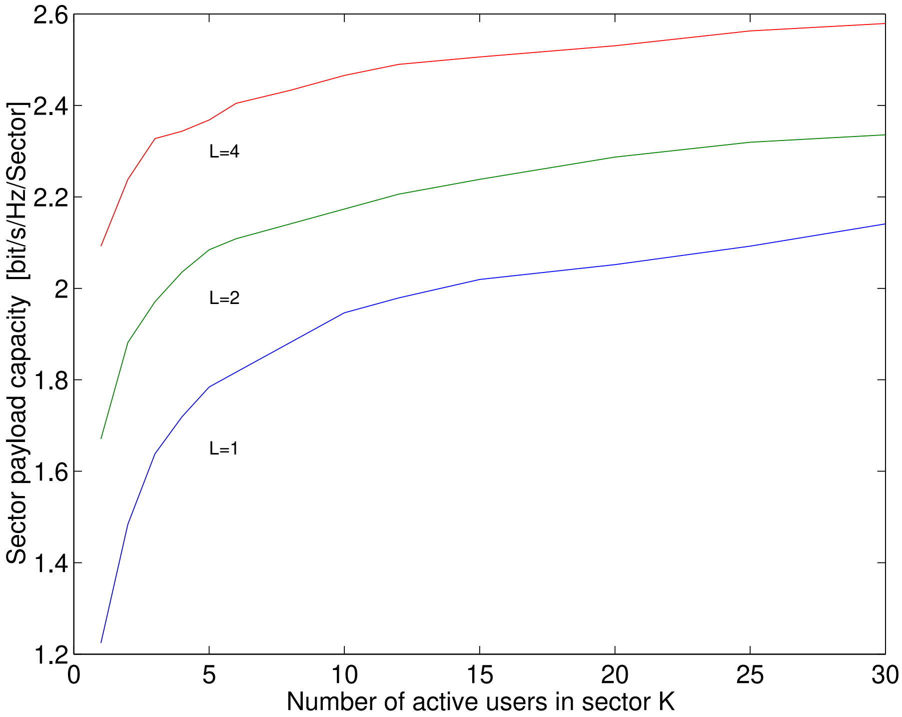

Figure 14: Estimated sector payload capacity for Rayleigh short-term fading, including all overhead and reuse factors, as a function of the number of active users K, who have L receiver antennas and use MRC combining. Each data point is based on $N = 10000$ realizations. The sector boundary is $d_1 = 0.7d = 0.61R$. The traffic load factor is $\ell = 1$ and the path loss exponent is $\alpha = 4$.

load capacity

$$C_{11s} \approx 0.811\ \bar{\eta}_s = 1.44 \quad \text{[bit/s/Hz/sector]}\ . \tag{24}$$

This represents the capacity for a single user within the sector (cell), with one antenna, who always has data to send, in an otherwise fully loaded system, averaged with respect to the location of the user. Only the path loss is taken into account, using a path loss exponent $\alpha = 4$.

For one user with *Rayleigh fading* channel within the diamond-shaped cell, we did in Section 8 for $d_1 = 0.6d$ obtain the corresponding estimates

$$\bar{\eta}_f = 1.525 \quad ; \quad C_{11f} \approx 0.811\bar{\eta}_f = 1.24 \quad \text{[bit/s/Hz/sector]}\ . \tag{25}$$

The estimate (25) includes retransmission overhead and the equivalent reuse factor $1/c_{\text{tot}} = 1.99$. The boost in sector payload capacity due to multiuser diversity and the use of $L > 1$ receiver antennas with MRC is shown in Figure 14. MIMO transmission over 2×2 channels would provide further improvements [4].

The sector capacity for $K = 5, L = 2$ would correspond to 10.5 Mbit/s per sector when using a 5 MHz bandwidth. According to this estimate, we would need a 48 MHz bandwidth to attain 100 Mbit/s sector capacity, combined with wide area coverage.

11 Conclusions and Open Issues

The scheme for interference avoidance proposed here accomplishes the task it was designed for: It assures that the whole sector, not only the area closest to the base station, can be covered without a large loss in spectral efficiency due to the frequency reuse scheme. The key idea is to apply a frequency reuse factor > 1 only where it is needed most, in the outer parts and along edges of the sector, where the signal from the base station is weak and interference is strong.

Can the design be improved? Very probably. A possible method is to apply the coordinated scheduling that is outlined in Section 3 not only to the sectors within each site, but also to the strongest interferers in other sites, perhaps coordinating all sectors of a 3-site reuse pattern. As we saw in Chapter 3, coordination does lower the attainable throughput, and it corresponds to an equivalent reuse factor at fully loaded sites. It could perhaps be seen as flexible method which improves performance and QoS in zone 1 for $\ell < 1$, when the system is not fully loaded.

When the traffic load varies between sites and sectors, as it will in practice, there should exist a method for adaptation of the resource partitioning into s_1 and s_2 that improves performance. Note, however, that the interference in zone 2 will increase when this partitioning is no longer the same over the whole system.

In the present proposal, users in the outer zone 2 are provided with only $1/3$ of the bandwidth as compared to users within zone 1. Could this be mitigated by power control, i.e. by increasing the downlink power when transmitting to users in zone 2? The answer is *no* in the present proposal in an interference-limited scenario. A power increase would also increase the interference level in proportion to the increased signal level, so the effects would cancel. If the reception quality is *noise-limited* in zone 2, the situation is different. We could then improve performance by increasing the transmission energy allocated to the band s_2. This is an important aspect which should be investigated further.

Another alternative that requires investigation is the use multiple receiver antennas for interference rejection. The works [10] and [11] by Bo Hagerman are relevant here. He investigated the relative strengths of interferers in downlinks in hexagonal and street-canyon environments, including reuse 3 patterns. In almost all cases the two dominating interferers contribute the major part of the energy. It might therefore be possible to attain good interference suppression by IRC with relatively few antennas in the user equipment *if* local scattering is not “rich”.

Finally, we have investigated the use of Trellis-coded modulation in our scheme. This resulted in an improvement roughly equivalent to lowering the rate boundaries γ_i by 1-2 dB, while the attained symbol error rate remained constant [12].

References

[1] The Wireless IP Project within the SSF PCC (Personal Computing and Communication) program
www.signal.uu.se/Research/PCCwirelessIP.html

[2] T. Ottosson, M. Sternad, A. Ahlén, A. Svensson and A. Brunström, "Towards a 4G IP-based wireless system proposal," *Radiovetenskap och Kommunikation RVK 02*, Stockholm, June 2002.
http://www.signal.uu.se/Publications/abstracts/c0206.html

[3] M. Sternad, T. Ottosson, A. Ahlén and A. Svensson, "The potential of multiuser diversity in adaptive OFDM downlinks".
Internal Report, SSF Wireless IP Project, July 2002.

[4] M. Sternad, "Transmit diversity and spatial multiplexing schemes for the OFDM downlink,"
Internal Report, SSF Wireless IP Project, September 2002.

[5] Li Chunjian, *Efficient Antenna Patterns for Three-Sector WCDMA Systems*. Master Thesis, Communication Systems Group, Department of Signals and Systems, Chalmers University of Technology, Report EX006/2003, February 2003.

[6] M.D. Yacoub, *Foundations of Mobile Radio Engineering*, CRC Press 1993.

[7] IEEE 802.16 Broadband Wireless Access Working Group: Channel models for fixed wireless applications. Report IEEE 802.16.3c-01/29r4, June 7, 2001.

[8] W.C.Y. Lee, *Mobile Cellular Telecommunications Systems*, McGraw Hill, New York, 1989.

[9] J.G.Proakis, *Digital Communications*, McGraw-Hill, New York, 4th edition, 2001.

[10] B. Hagerman, "Downlink relative co-channel interference powers in cellular radio systems," IEEE VTC 1995.

[11] B. Hagerman, "Strongest interferer adaptive single-user receivers in cellular radio environments," IEEE GlobeCom 1995.

[12] S. Falahati, M. Hong, A. Svensson and M. Sternad, "Adaptive Trellis coded modulation over predicted flat fading channels," *IEEE VTC 2003-Fall*, Orlando, Fla, Oct. 2003.

[13] W. Wang, T. Ottosson, M. Sternad, A. Ahlén and A. Svensson, "Impact of multiuser diversity and channel variability on adaptive OFDM," *IEEE VTC 2003-Fall*, Orlando, Fla, Oct. 2003.